Acta Crystallographica Section F
Structural Biology and Crystallization Communications
ISSN 1744-3091

Purification, crystallization and data collection of the apoptotic nuclease endonuclease G

Sei Mee Yoon,[a,b] Hyung Nam Song,[a] Jun Hyuk Yang,[a] Mi Yeon Lim,[a] Yong Je Chung,[b] Seong Eon Ryu[a,c] and Eui Jeon Woo[a]*

[a]Medical Proteomic Research Center, Korea Research Institute of Bioscience and Biotechnology, Daejeon 306-333, Republic of Korea, [b]Department of Biochemistry, Chungbuk National University, Cheongju 361-763, Republic of Korea, and [c]Systemic Proteomes Research Center, Korea Research Institute of Bioscience and Biotechnology, Daejeon 306-333, Republic of Korea

Correspondence e-mail: ejwoo@kribb.re.kr

Received 2 March 2009
Accepted 8 April 2009

Endonuclease G (EndoG) is a mitochondrial enzyme that responds to apoptotic stimuli by translocating to the nucleus and cleaving chromosomal DNA. EndoG is the main apoptotic endonuclease in the caspase-independent pathway. Mouse EndoG without the mitochondrial localization signal (amino-acid residues 1–43) was successfully overexpressed, purified and crystallized using a microbatch method under oil. The initial crystal (type I) was grown in the presence of the detergent CTAB and diffracted to 2.8 Å resolution, with unit-cell parameters a = 72.20, b = 81.88, c = 88.66 Å, β = 97.59° in a monoclinic space group. The crystal contained two monomers in the asymmetric unit, with a predicted solvent content of 46.6%. Subsequent mutation of Cys110 improved the stability of the protein significantly and produced further crystals of types II, III and IV with space groups $C2$, $P4_12_12$ (or $P4_32_12$) and $P2_12_12_1$, respectively, in various conditions. This suggests the critical involvement of this conserved cysteine residue in the crystallization process.

1. Introduction

Apoptosis is a physiological cell-death program that is essential for normal embryonic development, maintenance of tissue homeostasis and appropriate physiological response to tissue injury (David *et al.*, 2006). One hallmark of the terminal stages of apoptosis is internucleosomal DNA breakdown (Wyllie, 1980; Zhang & Xu, 2002; Widlak & Garrard, 2005). Upon activation of apoptosis, many apoptogenic factors, such as cytochrome *c*, procaspases, Smac/DIABLO, apoptosis-inducing factor (AIF) and EndoG, are released from the mitochondria (Yang *et al.*, 1997; Du *et al.*, 2000; Susin *et al.*, 1999).

Endonuclease G (EndoG) is a mitochondrial enzyme that responds to apoptotic stimuli by translocating to the nucleus and cleaving the chromosomal DNA in the caspase-independent pathway (Li *et al.*, 2001; Parrish *et al.*, 2001; Dupont-Versteegden *et al.*, 2006; Low, 2003). EndoG was originally purified from chicken erythrocyte nuclei as a mitochondrial endonuclease that has unique site selectivity and efficiently cleaves double-stranded DNA rich in C and G stretches (Ruiz-Carrillo & Renaud, 1987; Apostolov *et al.*, 2007). The EndoG nuclease is translated as a 33 kDa precursor protein, with the N-terminal 48 amino acids of the mitochondrial targeting sequence (MLS) being deleted during the translocation. The enzyme was initially thought to play a role in mitochondrial DNA replication (Cote & Ruiz-Carrillo, 1993; Huang *et al.*, 2002; Ikeda & Ozaki, 1997), although its function is now widely recognized to be the breakdown of chromosomal DNA during apoptosis in response to death stimuli such as truncated Bid, tumour necrosis factor α, UV irradiation and reactive oxygen species (ROS) (Li *et al.*, 2001; Parrish *et al.*, 2001; van Loo *et al.*, 2001).

EndoG belongs to a large family of DNA/RNA nonspecific nucleases with a $\beta\beta\alpha$-Me finger motif. This family of enzymes comprises nucleases that are well conserved throughout the range of microbial and eukaryotic organisms. The $\beta\beta\alpha$-Me finger motif is shared by a broad class of nucleases (Kuhlmann *et al.*, 1999) which includes the highly specific homing endonuclease I-PpoI (Flick *et al.*,

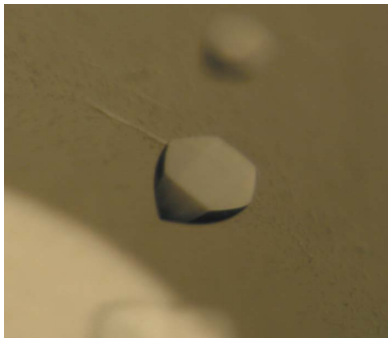

1998; Friedhoff, Franke, Meiss *et al.*, 1999; Friedhoff, Franke, Krause *et al.*, 1999), a member of the His-Cys box family (Belfort & Roberts, 1997) and the *Vibrio* nuclease Vvn from *V. vulnificus* (Wu *et al.*, 2001; Li *et al.*, 2003).

At physiological ionic strengths, EndoG is a poor endonuclease that degrades the efficiency of cleaved double-stranded (ds) DNA/RNA. It is thought to require nuclear proteins such as AIF, FEN-1 and Hsp70 (Widlak *et al.*, 2001; Kalinowska *et al.*, 2005) as additional cofactors to regulate its activity. Nuc1p, a yeast homologue of EndoG, has been reported to interact with karyopherin Kap123p for translocation and to bind to the phosphorylated histone H2B. The phosphorylation of histone H2B is known to be a necessary process in yeast EndoG-mediated apoptosis (Buttner *et al.*, 2007). Recently, a new endogenous inhibitor protein of EndoG was found in *Drosophila*. It is located in the cell nucleus to protect the cell from the chromosomal damage inflicted by EndoG (Temme *et al.*, 2009).

No crystal structures are available for this apoptotic nuclease from eukaryotes to date, despite detailed study of its biochemical properties and cellular functions. The *Anabaena* and *Serratia* nucleases are prokaryotic EndoGs that share 30% and ∼26% sequence identity to mouse EndoG, respectively, and their crystal structures have been determined. Structural information is available together with detailed mutational analyses for these two microbial enzymes, which are secreted nucleases involved in nucleotide salvage (Miller *et al.*, 1999; Ghosh *et al.*, 2005; Schafer *et al.*, 2004; Dake *et al.*, 1988). In the present study, the purification, crystallization and diffraction data collection of recombinant mouse EndoG expressed in *Escherichia coli* are reported. The X-ray crystal structure of the present protein is expected to reveal the structural features involved in the DNA-degradation mechanism upon stimulation of apoptosis.

2. Materials and methods

2.1. Cloning

For determination of the structure, a H138A mutation was made in the active site to allow optimal expression of the protein in *E. coli.* All attempts to subclone active EndoG into expression vectors other than those of the pET system (Novagen) led to spontaneous mutations in *E. coli* DH5a, suggesting that EndoG expression is deleterious to the cell, as previously reported (Cote & Ruiz-Carrillo, 1993). The expression vector of mouse EndoG containing the coding sequence for residues 44–293 without MLS was constructed using the pMAL-c2x vector (New England Biolabs). A Qiagen kit (Qiagen Sample and Assay Technologies) was used for the site-directed mutagenesis of Cys110 to alanine and DNA sequencing confirmed the absence of any undesired mutations.

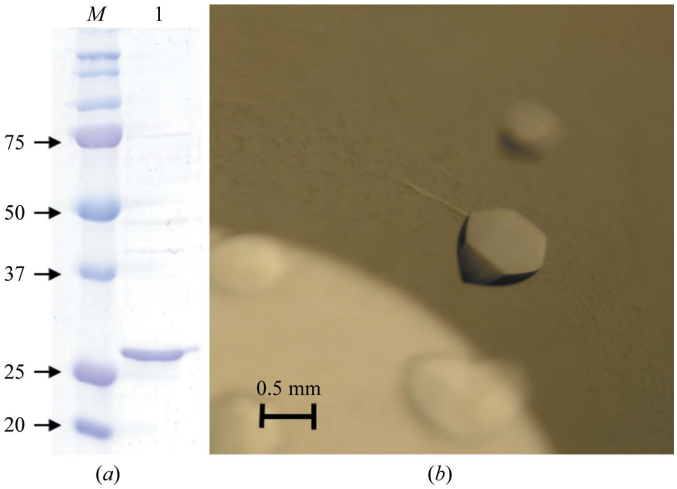

Figure 1
(*a*) SDS–PAGE gel showing purified mouse EndoG protein (∼29 kDa). Molecular-mass markers (kDa) are indicated on the left. (*b*) A single crystal of mouse EndoG (space group $P2_1$) grown by the microbatch method.

2.2. Expression and purification of recombinant mutant EndoG

The recombinant plasmid was transformed into *E. coli* strain BL21 (RIL). The transformed cells were then cultured at 310 K in LB medium containing 50 µg ml^{-1} ampicillin. When the culture density reached an OD (A_{600}) value of 0.7, protein expression was induced with 1 m*M* IPTG at 283 K for 2 d. The purification method described below was applied to both the H138A and C110A/H138A mutant proteins. Cells were harvested by centrifugation and resuspended in 30 m*M* sodium phosphate pH 7.5, 50 m*M* NaCl, 1 m*M* $MgCl_2$, 10 m*M* β-mercaptoethanol (β-ME) containing 5% glycerol (buffer *A*) and were then homogenized by sonication. Crude extracts were centrifuged at 16 500 rev min^{-1} for 1 h to remove aggregated proteins and cell debris. The supernatant of the cell lysates in buffer *A* was loaded onto an amylose column and the protein was eluted with the same buffer containing 20 m*M* maltose (buffer *B*). The N-terminal MBP tag was removed by TEV protease during dialysis (using a buffer containing 50 m*M* Tris–HCl pH 8.0, 50 m*M* NaCl, 10 m*M* β-ME, 1 m*M* $MgCl_2$, 5% glycerol; buffer *C*) and the protein sample was loaded onto a HiTrap-Q column. Fractions containing EndoG were pooled and then applied onto a HiTrap Heparin column. EndoG was eluted with a gradient of 0–0.5 *M* NaCl, dialyzed against buffer *C*, concentrated to 10 mg ml^{-1} and then used for crystallization. All columns were purchased from Amersham Biosciences. The purity of the EndoG protein was confirmed using 12% SDS–PAGE with Coomassie Brilliant Blue R-250 staining (Fig. 1*a*).

2.3. Crystallization

Four types of crystal were produced and refined. Type I contained the mutant protein H138A and types II–IV contained the C110A/H138A double-mutant protein. Crystallization trials of mouse EndoG were initially performed *via* a microbatch method under oil (Hampton Research) at 291 K. Droplets containing 1.5 µl protein solution were mixed with an equal volume of mother liquor. One condition yielded a small diamond-shaped crystal of type I and was further refined to 200 m*M* NaCl, 1 m*M* $CdCl_2$, 100 m*M* CHES buffer pH 8.5, 10 m*M* CTAB, 5% glycerol and 5% MPD. Type II–IV crystals were obtained *via* the sitting-drop method at 291 K. While several crystals were produced under similar conditions in the microbatch method, the double-mutant protein yielded better quality type II–IV crystals using the sitting-drop method than using the microbatch method. A type II crystal was grown using a reservoir consisting of 25% PEG 3350, 0.1 *M* HEPES pH 7.5 and 0.2 *M* ammonium sulfate. A type III crystal was grown from 30% PEG 4000 and 0.2 *M* ammonium sulfate. Finally, a type IV crystal grew from 12% PEG 8000, 0.1 *M* HEPES pH 7.5, 14% ethylene glycol and additive 28 (30% dimethyl sulfoxide).

2.4. Diffraction data collection

The crystals were cryocooled at 95 K using a cryoprotectant consisting of mother liquor supplemented with 20% glycerol to minimize radiation damage. Flash-cooled crystals were then mounted in a nitrogen stream. X-ray diffraction data were collected on a CCD

Table 1
X-ray diffraction and processing statistics for the four crystal forms of mouse EndoG.

Values in parentheses are for the highest resolution shell.

	Type I (H138A)	Type II (C110A/H138A)	Type III (C110A/H138A)	Type IV (C110A/H138A)
X-ray source	HFMX 4A	HFMX 4A	MXII 6C	MXII 6C
Resolution (Å)	29.9–2.80	30.0–3.00	30.0–2.38	30.0–3.00
Unique reflections	47942	18439	24381	7788
Completeness (%)	99.7 (98.0)	84.2 (71.6)	99.6 (95.8)	98.9 (99.3)
$R_{merge}(I)$ (%)	8.6 (40.5)	14.9 (29.2)	10.8 (43.3)	12.5 (30.8)
$I/\sigma(I)$	13.5 (3.2)	8.02 (3.0)	15.7 (3.6)	12.2 (3.8)
Space group	$P2_1$	$C2$	$P4_12_12$ (or $P4_12_12$)	$P2_12_12_1$
Unit-cell parameters (Å, °)	a = 72.20, b = 81.88, c = 88.65, β = 97.59	a = 88.60, b = 68.12, c = 163.36, β = 93.28	a = b = 68.59, c = 251.32, β = 90.00	a = 52.56, b = 71.86, c = 109.14, β = 90.00
No. of molecules in ASU	2 monomers	2 monomers	2 monomers	4 monomers

detector using synchrotron radiation with a wavelength of 0.97 Å on the HFMX 4A beamline for type I and II crystals and on the MXII 6C beamline for type III and IV crystals. Diffraction images were collected with an oscillation angle of 1° and an exposure time of 1 s per image in a nitrogen-gas stream at 95 K. All diffraction data were processed and scaled with the *HKL*-2000 program package (Otwinowski & Minor, 1997). The data-collection statistics are summarized in Table 1.

3. Results and discussion

Initial attempts to subclone the EndoG gene into several *E. coli* expression vectors all failed, resulting in spontaneous point mutations at various sites. Thus, a site-directed mutation was introduced into the active site of His138 in the DRGH motif of the $\beta\beta\alpha$ nuclease. Consequently, the mutant H138A was successfully subcloned into the expression vector, implying a toxic effect of the nuclease function on the host cell during cell proliferation (Ghosh *et al.*, 2005).

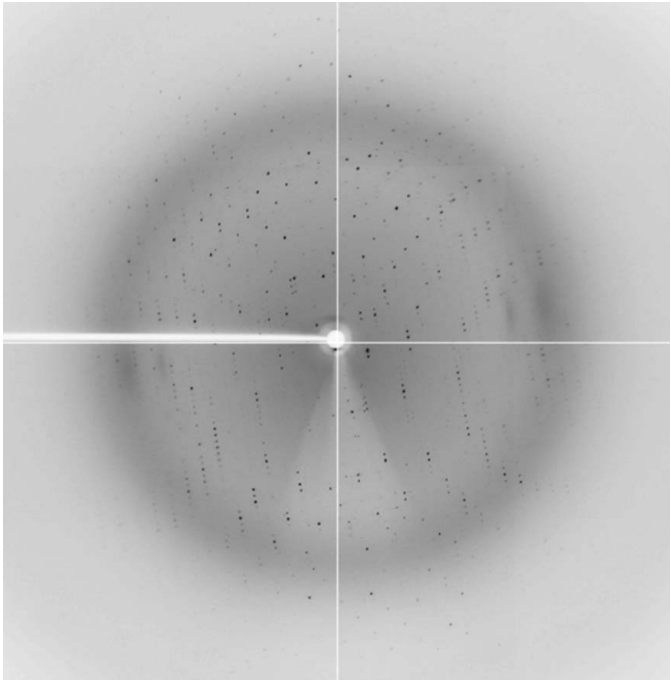

Figure 2
A typical diffraction pattern from a crystal of mouse EndoG (space group $P2_1$). The exposure time was 1 s, the crystal-to-detector distance was 250 mm and the oscillation range per frame was 1°.

Owing to the minimal expression and solubility level of variously tagged EndoGs, MBP-fusion EndoG in the absence of the mitochondrial localization signal (amino-acid residues 1–43) was used to improve the solubility and to facilitate the purification of the recombinant H138A protein. Induction of the EndoG H138A protein at low temperature effectively yielded a higher amount of soluble protein, whereas the protein was largely in the insoluble fraction after induction at 293 K. Throughout the entire purification process, EndoG H138A reacted sensitively to air oxidation, resulting in severe aggregation during purification. Accordingly, a high concentration of reducing reagent and the stabilizing reagent glycerol had to be added to prevent aggregation. Mg^{2+} ions were added to the buffer as EndoG is a metal-dependent enzyme and is known to stabilize active sites in microbial homologues (Miller *et al.*, 1999; Ghosh *et al.*, 2005).

The purified EndoG H138A protein was screened for crystallization using the microbatch method under oil. The initial crystal assumed the shape of a small diamond three months after crystallization setup with further optimization using additive screening (Fig. 1*b*). This type I crystal diffracted to 2.8 Å resolution (Fig. 2) on the PAL synchrotron beamline, with unit-cell parameters a = 72.20, b = 81.88, c = 88.66 Å, β = 97.59° in a monoclinic space group. The data-collection statistics are summarized in Table 1. The Matthews coefficient was calculated as 2.3 $Å^3$ Da^{-1} and the solvent content was 46.6% assuming the presence of two molecules in the asymmetric unit for the type I crystal.

Given that the EndoG H138A protein reacted sensitively to oxidation during purification and that the initial crystal was obtained a considerable amount of time after crystallization, oxidation of cysteine residues is likely to be involved in crystallization. Thus, the putatively reactive cysteine residues were also mutated. EndoG contains two cysteines: Cys110 and Cys193. Cys110 was identified as the mutation candidate, as Cys193 appears to be buried in the surface in the homology model constructed using the endonuclease template from *Serratia marcescens*. Surprisingly, the recombinant double-mutant C110A/H138A protein showed greatly improved stability during the purification process and subsequently yielded further crystals of types II, III and IV, with different space groups $C2$, $P4_12_12$ (or $P4_32_12$) and $P2_12_12_1$, respectively, under various conditions with a reduced time scale after crystallization setup. This result implies the critical involvement of cysteine residue Cys110 in both the crystallization process and in protein stabilization. Intriguingly, the apoptotic nuclease function of EndoG is triggered upon stimulation by reactive oxygen species inside the cell.

This study highlights a number of technical issues in the purification and crystallization of the toxic nuclease EndoG for structural study. Ongoing experiments will elucidate the structural features of EndoG that are involved in the mechanism of DNA degradation upon stimulation of apoptosis. Elucidation of the crystal structure of

mouse EndoG will also reveal the molecular characteristics of EndoG in eukaryotic organisms compared with homologous endonucleases in microorganisms, which do not have an apoptotic function.

We thank the beamline staff at HFMW 4A and MXII 6C, Pohang Accelerator Laboratory for data collection and technical assistance. This research was supported by a Korea Science and Engineering Foundation (KOSEF) grant funded by the Korean Government (MOST; No. R01-2007-000-20545-0).

References

Apostolov, E. O., Wang, X., Shah, S. V. & Basnakian, A. G. (2007). *Cell Death Differ.* **14**, 1971–1974.
Belfort, M. & Roberts, R. J. (1997). *Nucleic Acids Res.* **25**, 3379–3388.
Buttner, S., Eisenberg, T., Carmona-Gutierrez, D., Ruli, D., Knauer, H., Ruckenstuhl, C., Sigrist, C., Wissing, S., Kollroser, M., Frohlich, K. U., Sigrist, S. & Madeo, F. (2007). *Mol. Cell*, **25**, 233–246.
Cote, J. & Ruiz-Carrillo, A. (1993). *Science*, **261**, 765–769.
Dake, E., Hofmann, T. J., McIntire, S., Hudson, A. & Zassenhaus, H. P. (1988). *J. Biol. Chem.* **263**, 7691–7702.
David, K. K., Sasaki, M., Yu, S. W., Dawson, T. M. & Dawson, V. L. (2006). *Cell Death Differ.* **13**, 1147–1155.
Du, C., Fang, M., Li, Y., Li, L. & Wang, X. (2000). *Cell*, **102**, 33–42.
Dupont-Versteegden, E. E., Strotman, B. A., Gurley, C. M., Gaddy, D., Knox, M., Fluckey, J. D. & Peterson, C. A. (2006). *Am. J. Physiol. Regul. Integr. Comp. Physiol.* **291**, R1730–R1740.
Flick, K. E., Jurica, M. S., Monnat, R. J. Jr & Stoddard, B. L. (1998). *Nature (London)*, **394**, 96–101.
Friedhoff, P., Franke, I., Meiss, G., Wende, W., Krause, K. L. & Pingoud, A. (1999). *Nature Struct Biol.* **6**, 112–113.
Friedhoff, P., Franke, I., Krause, K. L. & Pingoud, A. (1999). *FEBS Lett.* **443**, 209–214.
Ghosh, M., Meiss, G., Pingoud, A., London, R. E. & Pedersen, L. C. (2005). *J. Biol. Chem.* **280**, 27990–27997.
Huang, K. J., Zemelman, B. V. & Lehman, I. R. (2002). *J. Biol. Chem.* **277**, 21071–21079.
Ikeda, S. & Ozaki, K. (1997). *Biochem. Biophys. Res. Commun.* **235**, 291–294.
Kalinowska, M., Garncarz, W., Pietrowska, M., Garrard, W. T. & Widlak, P. (2005). *Apoptosis*, **10**, 821–830.
Kuhlmann, U. C., Moore, G. R., James, R., Kleanthous, C. & Hemmings, A. M. (1999). *FEBS Lett.* **463**, 1–2.
Li, C. L., Hor, L. I., Chang, Z. F., Tsai, L. C., Yang, W. Z. & Yuan, H. S. (2003). *EMBO J.* **22**, 4014–4025.
Li, L. Y., Luo, X. & Wang, X. (2001). *Nature (London)*, **412**, 95–99.
Loo, G. van, Schotte, P., van Gurp, M., Demol, H., Hoorelbeke, B., Gevaert, K., Rodriguez, I., Ruiz-Carrillo, A., Vandekerckhove, J., Declercq, W., Beyaert, R. & Vandenabeele, P. (2001). *Cell Death Differ.* **8**, 1136–1142.
Low, R. L. (2003). *Mitochondrion*, **2**, 225–236.
Miller, M. D., Cai, J. & Krause, K. L. (1999). *J. Mol. Biol.* **288**, 975–987.
Otwinowski, Z. & Minor, W. (1997). *Methods Enzymol.* **276**, 307–326.
Parrish, J., Li, L., Klotz, K., Ledwich, D., Wang, X. & Xue, D. (2001). *Nature (London)*, **412**, 90–94.
Ruiz-Carrillo, A. & Renaud, J. (1987). *EMBO J.* **6**, 401–407.
Schafer, P., Scholz, S. R., Gimadutdinow, O., Cymerman, I. A., Bujnicki, J. M., Ruiz-Carrillo, A., Pingoud, A. & Meiss, G. (2004). *J. Mol. Biol.* **338**, 217–228.
Susin, S. A. *et al.* (1999). *Nature (London)*, **397**, 441–446.
Temme, C., Weissbach, R., Lilie, H., Wilson, C., Meinhart, A., Meyer, S., Golbik, R., Schierhorn, A. & Wahle, E. (2009). *J. Biol. Chem.* **284**, 8337–8348.
Widlak, P. & Garrard, W. T. (2005). *J. Cell. Biochem.* **94**, 1078–1087.
Widlak, P., Li, L. Y., Wang, X. & Garrard, W. T. (2001). *J. Biol. Chem.* **276**, 48404–48409.
Wu, S. I., Lo, S. K., Shao, C. P., Tsai, H. W. & Hor, L. I. (2001). *Appl. Environ. Microbiol.* **67**, 82–88.
Wyllie, A. H. (1980). *Nature (London)*, **284**, 555–556.
Yang, J., Liu, X., Bhalla, K., Kim, C. N., Ibrado, A. M., Cai, J., Peng, T. I., Jones, D. P. & Wang, X. (1997). *Science*, **275**, 1129–1132.
Zhang, J. & Xu, M. (2002). *Trends Cell Biol.* **12**, 84–89.